MOLECULAR AND CELLULAR BIOLOGY, Apr. 2000, p. 2466–2474 Vol. 20, No. 7
0270-7306/00/$04.00+0

Placental Failure in Mice Lacking the Mammalian Homolog of Glial Cells Missing, GCMa

JÖRG SCHREIBER, EVA RIETHMACHER-SONNENBERG, DIETER RIETHMACHER, ELISABETH E. TUERK, JANNA ENDERICH, MICHAEL R. BÖSL, AND MICHAEL WEGNER*

Zentrum für Molekulare Neurobiologie, Universität Hamburg, D-20246 Hamburg, Germany

Received 23 December 1999/Accepted 6 January 2000

The GCM family of transcription factors consists of *Drosophila melanogaster* GCM, an important regulator of gliogenesis in the fly, and its two mammalian homologs, GCMa and GCMb. To clarify the function of these mammalian homologs, we deleted GCMa in mice. Genetic ablation of murine GCMa (mGCMa) is embryonic lethal, with mice dying between 9.5 and 10 days postcoitum. At the time of death, no abnormalities were apparent in the embryo proper. Nervous system development, in particular, was not impaired, as might have been expected in analogy to *Drosophila* GCM. Instead, placental failure was the cause of death. In agreement with the selective expression of mGCMa in labyrinthine trophoblasts, mutant placentas did not develop a functional labyrinth layer, which is necessary for nutrient and gas exchange between maternal and fetal blood. Only a few fetal blood vessels entered the placenta, and these failed to thrive and branch normally. Labyrinthine trophoblasts did not differentiate. All other layers of the placenta, including spongiotrophoblast and giant cell layer, formed normally. Our results indicate that mGCMa plays a critical role in trophoblast differentiation and the signal transduction processes required for normal vascularization of the placenta.

Drosophila melanogaster Glial Cells Missing (GCM) (15, 18, 39) and its mammalian homologs, GCMa/GCM1 and GCMb/GCM2 (1, 3), form a small family of transcription factors. The defining feature of these proteins is a highly conserved domain in the amino-terminal region which has been referred to as the gcm box and constitutes the DNA-binding domain (1, 32). The close resemblance of the DNA-binding domains is also reflected in the very similar DNA-binding specificities of GCM proteins (31, 36). Additional structural features shared by GCM proteins include the presence of a transactivation domain in the extreme carboxy terminus and high turnover rates with half-lives ranging between 0.5 h (for GCMb) and 2 h (for GCMa) (29, 32, 36).

The function of *Drosophila* GCM is understood quite well. It is expressed in both the hemocyte lineage (8) and the developing nervous system (15, 18, 39). In the latter, GCM expression is restricted to prospective glial cells. In fact, GCM is by far the earliest marker for glial cells in *Drosophila*, and analysis of mutant flies has shown that GCM is both necessary and sufficient to induce glial fate in an uncommitted neural precursor (15, 18, 39). GCM thus functions as a master regulator of gliogenesis in *Drosophila*.

If one assumes that generation of glial cells from neural precursors is mediated by an evolutionarily conserved mechanism, one might expect that mammalian GCM homologs would also play a role in the generation of glial cells throughout the mammalian nervous system (4). Backing this hypothesis, ectopic expression of a GCMa transgene in the developing nervous system of *Drosophila* led to a significant increase in glial cells at the expense of neurons (21, 29). GCMb failed to cause a comparable neuron-to-glia transformation under similar experimental conditions (21).

However, expression of both GCMa and GCMb in the mammalian nervous system was detected only by sensitive PCR methods (3, 6, 21). The only site where expression of GCMb was readily detectable was the developing parathyroid (21). GCMa was primarily detected in the developing placenta (3, 6, 17, 21). Here, GCMa expression started early in the chorion (6). During development of the placenta, the chorion collapses onto the ectoplacental cone and fuses with the allantois to develop into the labyrinth. The labyrinth functions as the site of gas and nutrient exchange between fetal and maternal blood once the yolk sac circulation can no longer meet the increasing metabolic demand of the embryo. To that end, the labyrinth contains juxtaposed maternal blood sinuses and fetal blood vessels separated only by a three-cell-layered barrier of partially syncytial labyrinthine trophoblasts. Fetal blood vessels are derived from the allantoic mesenchyme, whereas the labyrinthine trophoblasts stem from the chorion. Trophoblasts of the labyrinth layer express murine GCMa (mGCMa), as do their chorionic precursors (6). Expression decreases only after 15.5 days postcoitum (d.p.c.) but remains detectable until 17.5 d.p.c.

Expression patterns of GCMa and GCMb are more compatible with a function of mammalian GCM proteins outside the nervous system. To clarify the function of mammalian GCM proteins, we deleted the GCMa gene by targeted mutagenesis in mice. Here we report that genetic ablation of GCMa leads to early embryonic lethality which results from placental defects, in particular from a failure of labyrinth layer formation.

MATERIALS AND METHODS

Construction of targeting vector. Genomic sequence from the GCMa locus of 129/Sv mice was obtained by screening a lambda phage library. A 2.2-kb *Not*I/*Nru*I PCR fragment starting in intron 1 and ending in exon 3 was used as 5′ homology region and was placed in front of a *lacZ* marker such that a continuous open reading frame was generated between the 32 amino-terminal residues of GCMa and LacZ. A 3.8-kb *Eco*RI fragment downstream of the known untranslated region of exon 6 was used as 3′ homology region. Both the combination of 5′ homology region and *lacZ* and the 3′ homology region were inserted in pPNT(37) on either side of the neomycin resistance cassette (Fig. 1A). The targeting vector thus replaced the complete open reading frame of GCMa downstream of amino acid 32 with a *lacZ* marker gene (Fig. 1B). The construct was linearized with *Not*I before electroporation.

* Corresponding author. Mailing address: ZMNH, Martinistr. 52, D-20246 Hamburg, Germany. Phone: 49 40 42803 6274. Fax: 49 40 42803 6602. E-mail: wegner@plexus.uke.uni-hamburg.de.

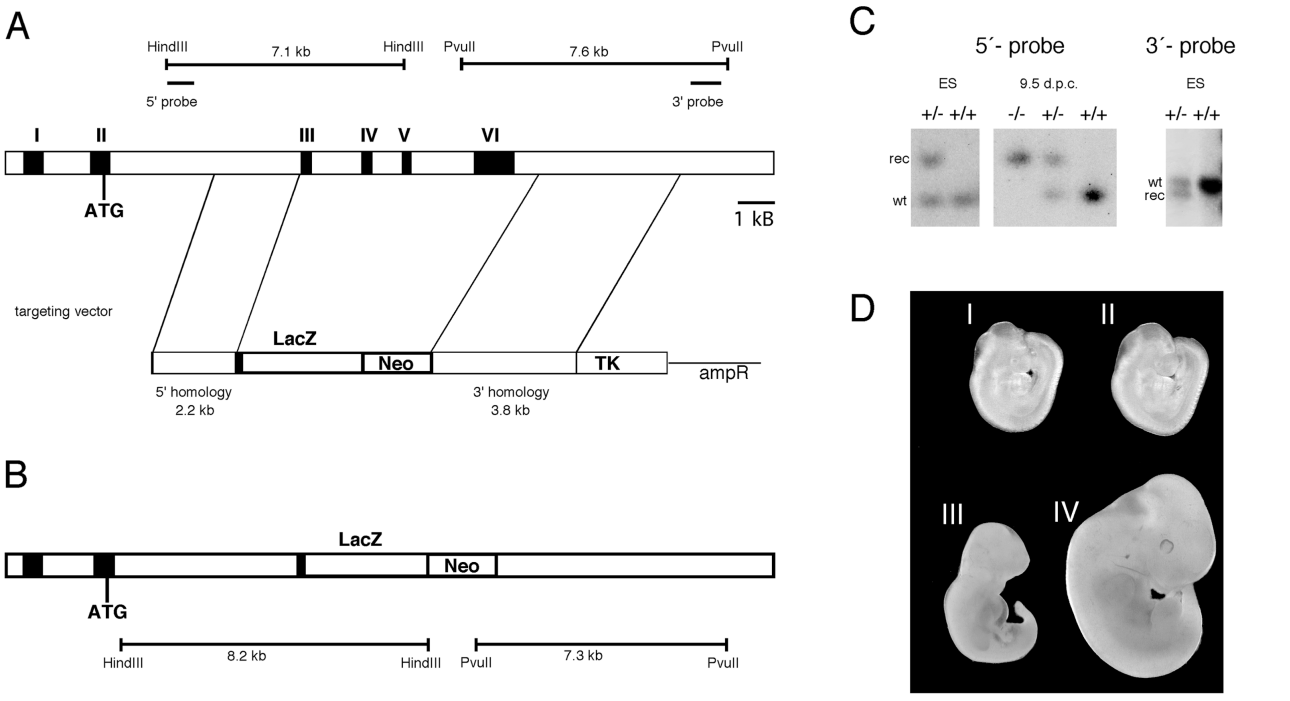

FIG. 1. Targeted disruption of mGCMa in mice. (A) Schematic representation of the mGCMa wild-type locus (top) and the targeting vector (bottom). mGCMa exons are marked by Roman numerals. (B) Targeted mGCMa allele. Localizations of the probes and the diagnostic restriction fragments before and after homologous recombination are shown. (C) Southern blot analysis of DNA from ES cells (ES) and 9.5-day-old mouse embryos (9.5 d.p.c.) digested with *Hin*dIII for use of the 5′ probe and *Pvu*II for use of the 3′ probe. The positions of bands corresponding to the wild-type allele (wt) and the targeted allele (rec) are indicated. (D) Macroscopic appearance of mutant (I and III) and wild-type (II and IV) embryos recovered at 9.5 (I and II) and 11.5 (III and IV) d.p.c.

Gene targeting and generation of mouse mutants. The linearized construct was electroporated into R1 embryonic stem (ES) cells which were then selected with G418 (200 μg per ml) and ganciclovir (2 μM). Selected ES cell clones were screened by Southern blotting with a 0.4-kb 5′ probe, which recognizes a 7.1-kb fragment in the case of the wild-type allele and an 8.2-kb fragment in the case of the targeted allele in genomic DNA digested with *Hin*dIII (Fig. 1A and B). Four clones among the 150 tested exhibited the pattern expected for homologous recombination of one allele. Appropriate integration of the 3′ end of the targeting construct was verified in the four positive clones using a 1.2-kb 3′ probe on *Pvu*II-digested ES cell DNA. This probe hybridized to a 7.3-kb fragment in the targeted allele as opposed to a 7.6-kb fragment in the wild-type allele (Fig. 1A and B). Hybridization with a *neo* probe confirmed that only a single integration event had occurred. Two targeted ES cell lines were injected into blastocysts to generate chimeras. Chimeric males from two independent clones transmitted the targeted allele to their offspring. No differences were detected between mice derived from the two different ES cell lines. Homozygous mutant embryos were generated by heterozygote intercrosses. Genotyping was routinely performed by PCR analysis using a common upper primer located at the border of intron 2 and exon 3 (5′CAGAACGTGAAAACGACTGACTGG3′) and two lower primers located within exon 3 (5′CACTCTGCTGCTTCTGTCTGGCTT3′) and *lacZ* (5′GATAGGTTACGTTGGTGTAGATGG3′), respectively. DNA was obtained from tail tips or, in the case of embryos, from yolk sacs. PCR was performed in 30-μl reaction mixtures containing standard buffer and 0.5 μM (each) primer. The cycling conditions consisted of an initial 2-min denaturing step at 94°C, followed by 35 cycles of 30 s at 94°C, 30 s at 65°C, and 30 s at 72°C. A 260-bp fragment was indicative of the wild-type allele, and a 350-bp fragment was indicative of the targeted allele.

In situ hybridization, *lacZ* staining, histology, and microscopy. Entire conceptus and placentas were isolated at 8.5 to 13.5 d.p.c. from staged pregnancies. Staining for β-galactosidase activity was performed essentially as described previously (14). After fixation for 2 h in 4% paraformaldehyde, material was incubated at 37°C in 1% X-Gal (5-bromo-4-chloro-3-indolyl-β-D-galactopyranoside) for 1 to 6 h.

For in situ hybridization, placentas were fixed overnight at 4°C in 4% paraformaldehyde, dehydrated, bleached, rehydrated, and embedded in 20% gelatin. After a second overnight fixation in 4% paraformaldehyde, placentas were sectioned on a vibrating-blade microtome (vibratome) (100 μm). Digoxigenin-labeled riboprobes were produced with a digoxigenin-RNA labeling kit (Roche Diagnostics). Whole-mount in situ hybridization on vibratome slices was performed essentially as described previously (41) with probes for Flt1 (23), germ cell nuclear factor (GCNF) (34), and Dlx3 (28).

For histological analysis, placentas were fixed overnight at 4°C in 4% paraformaldehyde, dehydrated, and embedded in Technovit 7100 resin (Kulzer); 6-μm sections were stained with eosin-hematoxylin or with eosin only in the case of prior β-galactosidase staining.

RESULTS

Targeted mutagenesis of mGCMa. The mGCMa gene was targeted by homologous recombination in R1 ES cells with a vector that replaced most of exon 3 as well as exons 4 to 6 with the *lacZ* open reading frame followed by a neomycin selection cassette (Fig. 1A). Transcription of the neomycin resistance gene was in the same direction as transcription of mGCMa, and insertion of the *lacZ* gene was such that its open reading frame was fused in frame with the amino-terminal 32 residues of mGCMa (Fig. 1B). Because all other mGCMa residues were removed, the resulting mutant allele is null. ES cell clones in which homologous recombination of one allele had occurred were identified by Southern blot analysis with probes flanking the sequence included in the targeting vector (Fig. 1C). Two independent recombinant ES cell clones were used to generate chimeric mice. Germ line transmission was achieved with chimeras from both ES cell clones as evident from Southern blots (Fig. 1C), and identical results were obtained with mice obtained from both ES cell clones.

Heterozygous mice were viable and fertile. In matings of heterozygous to wild-type mice, the mutant allele was detected in approximately 50% of progeny (data not shown). They exhibited no obvious phenotypic defects. These results suggest that heterozygosity of mGCMa is phenotypically inapparent and that mGCMa is not imprinted.

Matings of heterozygous pairs, however, did not generate any live births of homozygous mutant mice. Thus, loss of both mGCMa alleles is embryonic lethal. To identify the time of

TABLE 1. Genotyping of offspring from mGCMa heterozygous parents

Age (d.p.c.)	No. of offspring per type		
	Wild type	Heterozygous	Homozygous
8.5	2	5	1
9.5	14	27	11
10.5	9	14	10[a]
11.5	4	10	6[a]
12.5	4	4	1[a]
All	33	60	29

[a] Recovered embryos were dead.

death, embryos derived from heterozygous intercrosses were genotyped at various stages of gestation and phenotypically analyzed. At 9.5 d.p.c., homozygous embryos were detectable (Fig. 1C). They were alive and present in the expected Mendelian frequency (Table 1). Their phenotypic appearance was indistinguishable from that of wild-type and heterozygous littermates (Fig. 1D, I and II). Their yolk sac appeared histologically normal. At 10.5 d.p.c., homozygous embryos were still present in expected numbers but dead (Table 1). The number of somites in homozygous mutant embryos indicated that fetal death occurred between 9.5 and 10 d.p.c. No gross abnormalities were detectable in the embryo proper up to the time of death. At 11.5 d.p.c., the homozygous mutant embryos were already smaller and showed signs of resorption (Fig. 1D, III and IV).

At this developmental stage, no mGCMa expression could be detected in the embryo proper (data not shown). There is, however, a strong expression of mGCMa in parts of the developing placenta from 7.5 d.p.c. onwards (3, 6, 21). Expression is restricted to extraembryonic ectoderm, in particular chorionic trophoblast and later trophoblast cells of the labyrinth (6). Exclusive expression in trophoblasts and the absence of gross morphological abnormalities in mutant embryos at the time of their death pointed to a placental defect.

Placental morphology of mGCMa knockout mice. Gross morphological examination of the placenta at 8.5 d.p.c. revealed no significant difference between homozygous mutant and wild-type mice (Fig. 2A and B). The chorion had collapsed onto the ectoplacental cone, and fusion between chorion and allantois had occurred. At this level of resolution, mutant placentas still looked fairly normal at 9.5 d.p.c. (Fig. 2C and D). By 10.5 and 11.5 d.p.c., abnormalities were clearly evident in the mutant placenta. The wild-type placenta had acquired the typical three-layered appearance with the labyrinth layer being the inner layer, the spongiotrophoblast being the middle layer, and the giant cells forming the outer layer and interface with the maternal decidua (Fig. 2F and H). Spongiotrophoblast and giant cell layer appeared normal in the homozygous placenta. The region corresponding to the labyrinth layer, however, exhibited a severe reduction in thickness (Fig. 2E and G). The overall shape of the placenta had changed due to the substantial size reduction of the labyrinth such that the majority of mutant placentas after being cut in half had a convex rather than a concave shape.

A more detailed histological analysis under higher magnification confirmed and extended these observations (Fig. 3). At higher resolution, defects became apparent earlier. At 9.5 d.p.c., chorionic trophoblasts were found densely packed at the base of the placenta in homozygous mutant embryos (Fig. 3A), whereas chorionic trophoblasts in age-matched wild-type

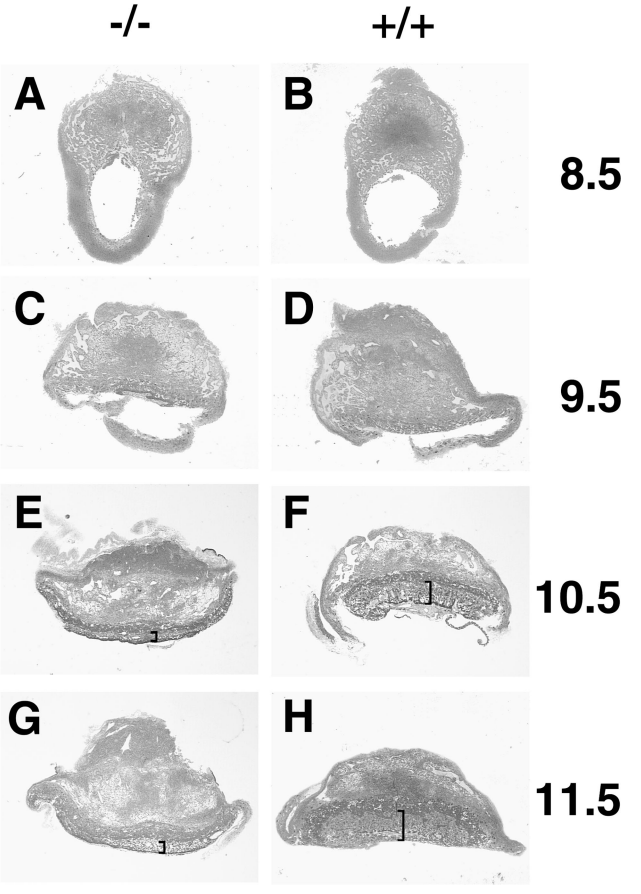

FIG. 2. Effects of mGCMa ablation on placental morphology. Transverse sections (6 μm) of Technovit-embedded placentas stained with eosin-hematoxylin at low magnification. (A, C, E, and G) Mutant. (B, D, F, and H) Wild type. (A and B) 8.5 d.p.c. (C and D) 9.5 d.p.c. (E and F) 10.5 d.p.c. (G and H) 11.5 d.p.c. The labyrinth layer is marked by brackets. Note the altered shape of the mutant placenta at later stages.

and heterozygous placentas had already started to spread inwards and participate in the formation of the labyrinth layer together with the angiogenic allantoic mesenchyme (Fig. 3B). Fetal blood vessels, identified by their containing nucleated embryonic blood cells, started entering the prospective labyrinth from the base. Their number was strongly reduced in mutant placentas compared to normal placentas (compare Fig. 4A to B). Those fetal blood vessels that were detected in the mutant were either outside the placenta or—when in the placenta—had formed exclusively near the base where the surrounding trophoblast tissue was very compact (Fig. 4A). In contrast to the normal placenta (compare with Fig. 4B), fetal blood vessels in the mutant placenta were never found in the immediate vicinity of maternal blood sinuses. These developed normally. The tight apposition of fetal blood vessels and maternal sinuses seen in the normal placenta is, however, a key prerequisite for the function of the labyrinth in the exchange of gas and nutrients between fetal and maternal blood.

At 10.5 d.p.c., the typical structure of the labyrinth was already visible in wild-type mice (Fig. 3D). In homozygous mutant mice, there was a drastic reduction in the size of this layer, and the number of cells in the mutant layer was decreased. The lower cell number and the invading maternal blood sinuses had given parts of the layer a sponge-like appearance (Fig. 3C). Near the base of the placenta, the layer

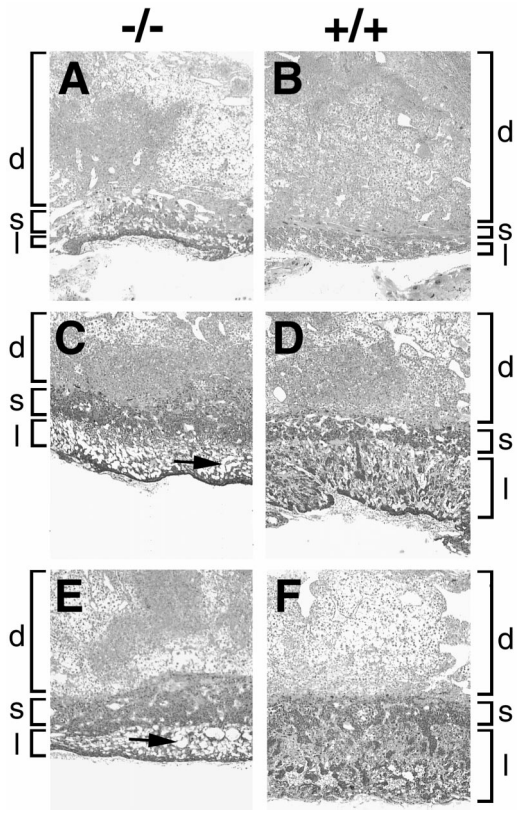

FIG. 3. Effects of mGCMa ablation on placental histology. Higher magnification of transverse sections (6 μm) of Technovit-embedded mutant (A, C, and E) and wild-type (B, D, and F) placentas at various developmental ages. (A and B) 9.5 d.p.c. (C and D) 10.5 d.p.c. (E and F) 11.5 d.p.c. Localizations of labyrinth layer (l), spongiotrophoblast layer (s), and maternal decidua (d) are indicated. Large cell-free areas in the abnormal labyrinth layer of the mutant are marked by arrows.

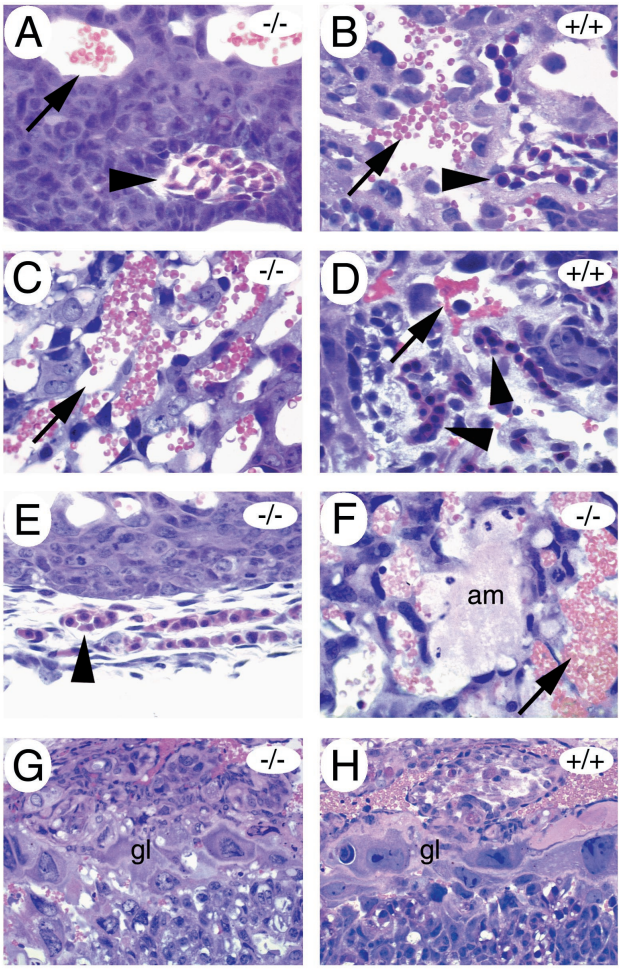

FIG. 4. Placental anomalies in mGCMa-deficient conceptus. Transverse sections (6 μm) of Technovit-embedded placentas. At 9.5 d.p.c. (A and B), few fetal blood vessels (arrowheads) were found within the prospective labyrinth of the mutant placenta (A) compared to the wild-type placenta (B). Maternal blood sinuses (arrows) were present in normal numbers but were never close to embryonal vessels at any time during development as observed for the wild type (B and D). At 10.5 d.p.c. (C to E), fetal blood vessels (arrowheads) were present in the labyrinth of normal placentas (D) but absent from the mutant (C) and were detected only outside the placenta (E). Amorphous material (am) was frequently deposited within the labyrinth layer of mutant placentas (12.5 d.p.c. in panel F). Giant cells (gl) are indistinguishable between mutant (G) and wild type (H) at 10.5 d.p.c. and later stages of development.

remained compact. By 10.5 d.p.c., fetal blood vessels were completely missing from mutant placentas, whereas an intricate network of fetal blood vessels had developed in juxtaposition to maternal blood sinuses in normal placentas (compare Fig. 4C to D). In the homozygous mutant, fetal blood vessels were detected only on the outside of the placenta underlying the compact layer of chorionic trophoblasts (Fig. 4E). The elongated differentiated trophoblasts that form the hemotrichorial barrier around the fetal blood vessels were undetectable in the mutant placenta. With increasing developmental age, amorphous material was detected throughout the mutant placenta (shown for 12.5 d.p.c. in Fig. 4F). Such deposits were absent from normal placentas. Even at this level of resolution, the giant cell layer (Fig. 4G and H) and the spongiotrophoblast layer appeared normal. If anything, there might have been a slight hypertrophy of the spongiotrophoblast layer (Fig. 3C to F).

As shown for 11.5 d.p.c., the same defects became even more pronounced at later points in development with the labyrinth layer growing significantly in size in normal placentas (Fig. 3F) but keeping a constant size in mutant placentas (Fig. 3E). We conclude from these observations that a functional labyrinth layer never forms in the mutant and that the resulting failure to supply the embryo with nutrients and oxygen is responsible for the observed embryonic lethality.

Analysis of trophoblast marker gene expression in mutant placentas. For a better characterization of the placental defect, we next compared the expression of several trophoblast markers in mutant and normal placentas (Fig. 5). From 9.5 d.p.c. onwards, the receptor tyrosine kinase Flt1 is a marker for the spongiotrophoblast (23). At all embryonic stages examined, Flt1 expression was very similar in normal and mutant placentas (Fig. 5B, E, H, K, N, and Q). In agreement with morphological analysis, the Flt1-positive spongiotrophoblast layer seemed on average slightly enlarged in mutant placentas.

Two markers were employed to study the labyrinth layer, in particular its trophoblast component. Both the orphan nuclear receptor GCNF and the mammalian *Distal-less* homolog Dlx3 are expressed in overlapping, but not identical, subsets of labyrinthine trophoblast cells (28, 34). At 9.5 d.p.c., cells expressing Dlx3 or GCNF were detected in normal and mutant placentas. In mutant placentas (Fig. 5A and C), they were arranged in a more compacted layer than in normal placentas (Fig. 5D and F). By 10.5 d.p.c., the area with Dlx3- and GCNF-

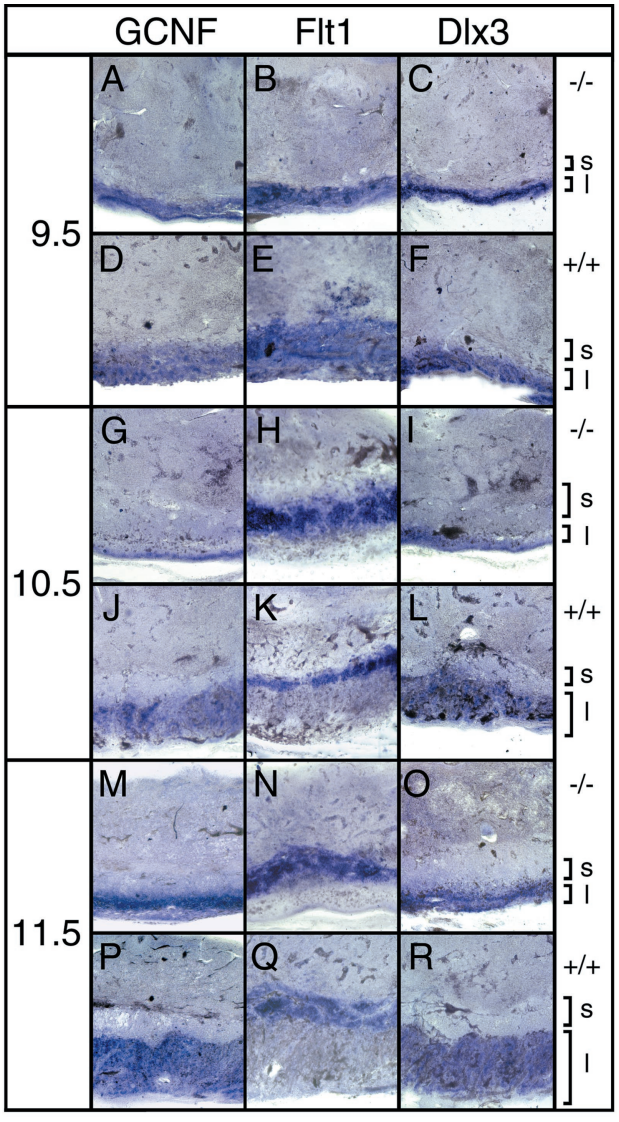

FIG. 5. Expression of placental markers. Transverse sections (100 μm) of paraformaldehyde-fixed placentas were hybridized with GCNF, Flt1, and Dlx3 probes as indicated. Analyzed were mutant (A to C, G to I, and M to O) and wild-type (D to F, J to L, and P to R) placentas from 9.5 (A to F), 10.5 (G to L), and 11.5 (M to R) d.p.c. Localizations of spongiotrophoblast (s) and labyrinth layer (l) are indicated.

expressing cells had expanded substantially in the normal placenta as expected for the labyrinth layer (Fig. 5J and L). The speckled distribution of the hybridization signal indicated that within the labyrinth Dlx3- and GCNF-positive trophoblasts had intermingled with Dlx3- and GCNF-negative cells derived from the allantoic mesenchyme. In contrast, Dlx3- and GCNF-expressing cells had remained in a narrow, compact layer in mutant placentas (Fig. 5G and I). Staining of this layer was uniform, indicating the absence of significant numbers of interspersed cells which did not express Dlx3 or GCNF. This layer corresponded to the densely packed chorionic trophoblasts at the base of the placenta but also contained material from the sponge-like structure between chorionic trophoblast layer and spongiotrophoblast, as this structure is not preserved during vibratome sectioning. These phenotypic changes were even more apparent at 11.5 and 12.5 d.p.c. (Fig. 5M to R and data not shown), indicating that the observed defect is of permanent rather than transient nature. In agreement with histological analyses, these results indicate that a typical labyrinth structure never formed. Chorionic trophoblasts as defined by expression of typical markers were, however, present in significant numbers in the absence of mGCMa expression.

Analysis of β-galactosidase expression in mutant placentas. Inclusion of the *lacZ* coding sequence in our target construct and its in-frame fusion with the amino terminus of mGCMa allowed us to monitor the fate of mGCMa-expressing cells in heterozygous normal and homozygous mutant placentas by β-galactosidase staining (Fig. 6). β-Galactosidase activity was already detected in chorionic trophoblasts around the time of chorion-allantois fusion in both mutant and normal placentas (Fig. 6A and B and data not shown). In the heterozygous placenta, β-galactosidase-expressing cells increased steadily in

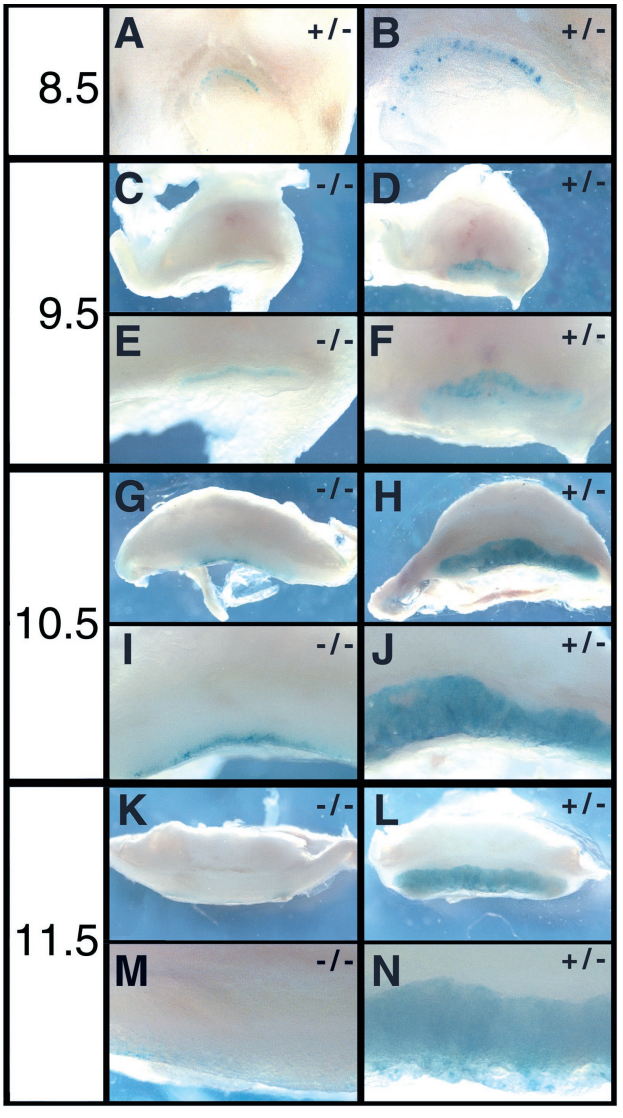

FIG. 6. β-Galactosidase staining of normal and mutant placentas. Paraformaldehyde fixed placentas were transversely cut in half at 8.5 (A and B), 9.5 (C to F), 10.5 (G to J), and 11.5 (K to N) d.p.c. and stained for β-galactosidase activity. A view from the sectioned side is shown in low (A, C, D, G, H, K, and L) and high (B, E, F, I, J, M, and N) magnification for both heterozygous normal (A, B, D, F, H, J, L, and N) and homozygous mutant (C, E, G, I, K, and M) placentas.

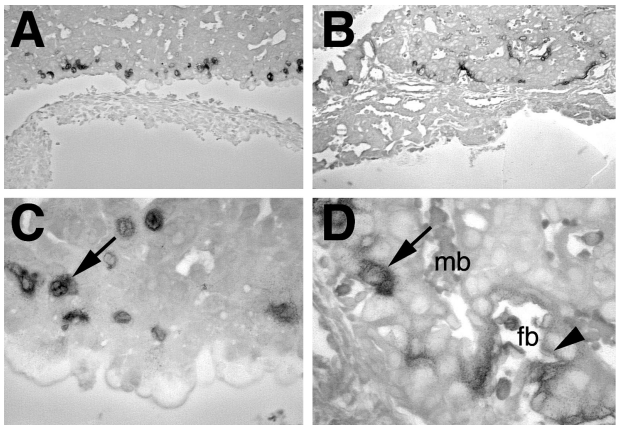

FIG. 7. High-resolution mapping of *lacZ*-expressing cells in the placenta. Close microscopic examination of 6-μm sections from *lacZ*-stained placentas at 10.5 d.p.c. counterstained with eosin. (A and C) Homozygous mutant placenta; (B and D) heterozygous normal placenta. Cuboidal mononuclear cells are marked by arrows, and syncytial trophoblasts close to fetal blood vessels are marked by arrowheads. mb, maternal blood sinus; fb, fetal blood.

number up to 11.5 d.p.c. and were spread over the whole area of the labyrinth (Fig. 6D, F, H, J, L, and N). Variations in staining intensities in different parts of the labyrinth indicated that β-galactosidase expression was not uniform throughout this layer, as already reported for GCNF and Dlx3 (Fig. 5). This expression pattern is caused by selective β-galactosidase expression in trophoblasts of the labyrinth and is very similar to the in situ hybridization pattern observed for mGCMa. We conclude that our *lacZ* marker faithfully mimicks the temporal and spatial expression of mGCMa in the developing placenta.

Closer microscopic examination on thin sections indeed confirmed that *lacZ* is not expressed in mesenchymal components of the labyrinth layer (Fig. 7B and D). In agreement with previous in situ hybridization results using an mGCMa probe (6), β-galactosidase was detected in two morphologically distinct types of labyrinthine trophoblast (Fig. 7D). The first were cuboidal mononuclear cells. The second were elongated cells of the three-cell-layered hemotrichorial barrier between fetal blood vessels and maternal blood sinuses. Of the three layers, the two closest to the fetal blood vessels consist of syncytial trophoblasts whereas the layer closest to the maternal sinuses is cellular. β-Galactosidase activity was higher in the syncytial trophoblasts closest to the fetal blood vessels and comparatively lower in the cellular trophoblasts lining the maternal blood sinuses. Expression in syncytial trophoblasts was also corroborated by the diffuse appearance of the β-galactosidase staining pattern. *lacZ* expression in the labyrinth layer remained strong until 12.5 d.p.c., which was the last developmental age analyzed in our study.

Mutant placentas exhibited a vastly different *lacZ* expression pattern. From 9.5 d.p.c., *lacZ*-expressing cells were strongly reduced (Fig. 6C and E). Those *lacZ*-expressing cells that were still present remained in the compact layer close to the base of the placenta and did not spread into the prospective labyrinth layer. Intriguingly, there were significantly fewer *lacZ*-expressing cells than GCNF- and Dlx3-expressing cells in the mutant placenta, indicating that mGCMa is not essential for obtaining the trophoblast fate. Up until 10.5 d.p.c., the *lacZ* expression remained fairly stable, despite the fact that the placenta increased dramatically in size during that same period (Fig. 6G and I). Thus, *lacZ*-expressing cells persisted in the mutant placenta until 10.5 d.p.c. or even slightly increased in number. From 11.5 d.p.c. onwards, however, *lacZ* expression was hardly detectable despite significant levels of Dlx3 and GCNF (Fig. 6K and M). Close inspection of thin sections furthermore revealed that the *lacZ*-expressing cells in the mutant placenta were confined to the compact layer at the inner side of the placenta (Fig. 7A and C). They corresponded exclusively to mononuclear, cuboidal cells, in agreement with the fact that differentiated elongated trophoblasts were not detected in the mutant placenta.

DISCUSSION

In this paper, we describe the result of targeted deletion of the mGCMa gene. mGCMa is one of the two mammalian homologs of the *Drosophila* GCM gene that have been identified in extensive searches over the last several years (1, 3, 6, 19–21, 31). Interest in these mammalian GCM homologs stemmed from the expected role of these proteins as master regulators of gliogenesis in mammals (4). The *Drosophila* GCM had previously been shown to be the earliest regulator involved in fate determination of glial cells (15, 18, 39). GCM proved to be quite potent in that function as ectopic expression of GCM resulted in transformation of cell fate towards a glial fate, whereas loss of GCM expression invariably led to an extensive loss of glial cells in both peripheral and central nervous systems and a concomitant increase in neurons (2, 7, 15, 18, 39).

Given the fact that homologous proteins often have conserved functions between species, it was expected that at least one of the two mammalian GCM homologs has a role in gliogenesis. Biochemical analyses and overexpression studies in flies indicated that GCMa was a better candidate than GCMb. For one thing, GCMa behaved much more like GCM in transfection studies than did GCMb (29). Additionally, GCMa was able to transform cells in the *Drosophila* embryo to cells with a glial phenotype, whereas GCMb failed to do so (21, 29).

Thus, we were surprised by the result of genetic mGCMa ablation. Instead of a defect in nervous system development, we obtained a severe placental defect that led to early embryonic lethality between 9.5 and 10 d.p.c. At the time of death, no major defects were detectable in the development of the nervous system or any other parts of the embryo proper. In effect, we were unable to detect expression of mGCMa in any part of the embryo including the nervous system either by in situ hybridization or by *lacZ* staining up until 13.5 d.p.c., which was the latest developmental stage analyzed in this study. Currently, we cannot exclude a role of mGCMa in later stages of nervous system development. This can be answered only by tetraploid aggregation experiments. However, if there is a role in nervous system development, it cannot be the one of a master regulator or an early determination switch, because glial progenitors are already formed and recognizable by marker gene expression at 13.5 d.p.c. both in the peripheral and in the central nervous system, i.e., at a time when mGCMa expression cannot be detected in the embryo proper. Thus, mGCMa does not seem to belong to those genes, in which function has been conserved during evolution.

In other respects, the placental phenotype was not unexpected, as this is the only tissue in which significant mGCMa expression had been detected by in situ hybridization analysis (6, 21). mGCMa expression has been reported for extraembryonic ectoderm of the chorion as early as 7.5 d.p.c. (6). Later, mGCMa expression is confined to the labyrinth layer of the placenta and therein to labyrinthine trophoblasts. Allantois-derived mesenchyme scores negative for mGCMa. The laby-

rinthine trophoblasts form a heterogenous population with two morphologically distinct cell types, cuboidal mononuclear cells which are believed to possess stem cell character (35) and elongated cells that separate fetal vessels and the maternal blood sinuses and are believed to represent the differentiated labyrinthine trophoblast stage. mGCMa is expressed in both the cuboidal and the elongated cells. This mGCMa expression pattern is faithfully recapitulated by the *lacZ* marker that we integrated into the mGCMa locus as part of our gene targeting strategy down to the cellular level. We first observed *lacZ* expression in the chorion around the time of chorion-allantois fusion. Later on, the *lacZ* marker was exclusively expressed in the trophoblast cells of the labyrinth. In heterozygous normal placentas, we detected it in both cuboidal and elongated labyrinthine trophoblasts. Thus, we believe that our *lacZ* marker will provide a useful tool to study fate and lineage relationships of labyrinthine trophoblasts. We can also conclude from our observation that no essential regulatory regions are present between exon 3 and exon 6 of mGCMa, as loss of this region did not interfere with correct spatial and temporal expression of the *lacZ* marker.

In accord with the strong and selective expression of mGCMa in the labyrinth, we found a major defect in labyrinth layer formation in the mGCMa knockouts which impaired chorioallantoic circulation. This defect is sufficient to explain the observed embryonic lethality. Due to their growing size, mouse embryos start to depend on the chorioallantoic circulation at 9.5 to 10 d.p.c., the exact time of death of the homozygous mutant embryos.

The defect in the labyrinth layer is not due to the loss of either chorion or allantois. In fact, both form normally. Thus, the defect in mGCMa knockouts occurs at a later stage than the one in the Ets2 knockout, in which there are no detectable chorion and allantoic membranes (22). Chorion and allantois were not only present; they also fused. Chorion-allantois fusion is an important prerequisite for formation of the labyrinth layer which is disturbed in a number of other mouse models with placental defects including knockouts for vascular cell adhesion molecule 1, α4 integrin, Mrj, and the nuclear orphan receptor Err2/Errβ (12, 16, 25, 42).

Following chorion-allantois fusion, the labyrinth layer forms with allantoic mesenchyme invading the placenta, forming the fetal blood vessels, and trophoblasts forming the three-cell-layered hemotrichorial barrier which separates fetal blood vessels and maternal blood sinuses and mediating the nutrient exchange. We observed severe anomalies in the establishment and maintenance of the fetal vascular network in the mGCMa knockouts. Allantoic blood vessels invaded the chorion in already dramatically reduced numbers, remained near the base of the placenta, and failed to elaborate into the vascular network typical of the labyrinth layer. By 10.5 d.p.c., fetal blood vessels were essentially absent from the mutant placenta and were detected only on the outside of the placental base.

In the normal placenta, trophoblasts and mesenchyme are not only intricately intertwined within the labyrinth layer; they also influence each other's development. Allantoic blood vessels induce the differentiation of the labyrinthine trophoblasts into cells of the hemotrichorial barrier (13, 38). Labyrinthine trophoblasts, on the other hand, express important mitogens required for normal vasculogenesis such as vascular endothelial growth factor (9). Defects in trophoblasts can therefore affect the development of the allantoic mesenchyme (33) and vice versa (38). With the absence of allantoic mesenchyme in the prospective labyrinth of mGCMa-deficient mice, trophoblasts failed to differentiate into the hemotrichorium that normally surrounds the fetal blood vessels. Instead, trophoblasts remained densely packed except in those regions invaded by maternal blood sinuses. Although there was a clear reduction in trophoblasts, significant numbers remained present and detectable.

Other processes which take place in the developing placenta, such as the formation of the secondary giant cells and the spongiotrophoblast from the ectoplacental cone, remained unaltered. If anything, there might have been a slight increase in the size of the spongiotrophoblast as indicated both by histological analysis and by in situ hybridization with a spongiotrophoblast-specific probe. However, given the fact that mGCMa was not found to be expressed in the spongiotrophoblast at any time of development, it seems likely that possible minor effects on spongiotrophoblast development are non-cell-autonomous and secondary to defects in the labyrinth layer.

Other mouse mutants have been described that exhibit defects in labyrinth layer formation. In the Mash-2 mutant, for instance, the labyrinth is not properly vascularized (11). However, in this case, it was shown that the labyrinth defect is secondary to a failure of the spongiotrophoblast to form because of the defective development of diploid stem cells in the ectoplacental cone (35).

In the RXRα-RXRβ double knockouts, the defect is intrinsic to the labyrinth layer (40). In this case, a markedly decreased proliferation and hence shortage of diploid trophoblast cells is responsible for labyrinth agenesis. After deletion of the Von Hippel-Landau tumor suppressor, allantoic vessels fail to enter the chorion altogether (10).

The phenotype of Dlx3-deficient mice shares obvious similarities to the phenotype described here for mGCMa in the time of embryonic death, the reduced vascularization, and the compact morphology of the labyrinth (28). The similarities in phenotypes are not unexpected, as both transcription factors are expressed in the same cell type in a temporally and spatially overlapping pattern. However, there are also differences between the two types of knockout mice. In addition to the labyrinth defect, Dlx3-deficient mice show a severe reduction in the size of the spongiotrophoblast layer, which was unaffected or even increased in size after genetic ablation of mGCMa. Furthermore, we never observed in GCMa-deficient mice the alterations in marker gene expression described in reference 28 for the Dlx3 knockouts. These phenotypic differences are paralleled by differences in expression. Especially during early phases of labyrinth formation, there are many more trophoblasts expressing Dlx3 than GCMa, with GCMa expression increasing only at later times. Thus, Dlx3 expression is possible in the absence of GCMa, arguing that both transcription factors are regulated differently in the same group of cells and likely perform separate functions.

Mice deficient for nuclear receptor PPARγ and the basic helix-loop-helix transcription factor Tfeb have the phenotype most similar to our GCMa knockout mice (5, 33). Fetal blood vessels invade the placenta, but rarely. Significant numbers of chorionic trophoblasts remain detectable, but they fail to undergo terminal differentiation in the vicinity of the fetal blood vessels. Maternal blood sinuses are dilated. No functional labyrinth forms. At present, it is unclear whether GCMa, Tfeb, and PPARγ are members of the same differentiation pathway and whether they are coordinately regulated during trophoblast differentiation. Expression studies of PPARγ and Tfeb in the mGCMa knockout (and vice versa) will clarify this issue.

Clearly different from the effects of mGCMa ablation are the phenotypic manifestations of Esx1, Wnt-2, and hepatocyte growth factor/scatter factor (HGF/SF) knockouts (24, 27, 30, 38). Compared to mGCMa, their effects become apparent only at later times of embryonic development. The defects in the

labyrinth layer are less severe. In the HGF/SF knockout, there is a shortage of labyrinthine trophoblasts and a concomitant increase of allantoic mesenchyme. As a consequence of this unbalance, formation of the hemotrichorial barrier from trophoblasts is disturbed (38). In the case of Esx1 and Wnt-2, the fetal vasculature is affected, with reduced numbers of fetal capillaries in the Wnt-2 knockout and aberrant branching patterns in the Esx1 knockout (24, 27). In both latter cases, the placenta is edematous and contains large pools of maternal blood. In the Esx1-deficient mice, wedges of spongiotrophoblast reach deep into the labyrinth layer, while giant cells can be found in the Wnt-2 knockouts throughout the labyrinth all the way to the chorionic plate. Comparable breaches of layer integrity have never been observed in the mGCMa knockout.

What could be the function of mGCMa in trophoblasts? As already mentioned, the pattern of mGCMa expression in chorionic and later in labyrinthine trophoblasts is not indicative of a role as a master regulator of the trophoblast fate. There are many more cells that are positive for the trophoblast-specific markers Dlx3 and GCNF in the early placenta than there are mGCMa-expressing cells. Also, trophoblast fate is maintained in the absence of mGCMa as evident from the persistence of significant numbers of Dlx3- and GCNF-positive cells in the mutant placenta.

Strikingly, mGCMa expression in labyrinthine trophoblasts correlated well with their proximity to allantoic mesenchyme. At the time of chorion-allantois fusion, all mGCMa-expressing cells were found in the chorionic plate in close contact with the allantois. In the Mrj mutant, loss of chorioallantoic fusion correlated with a strong reduction in mGCMa expression (16). Later, mGCMa-expressing cells started to appear in inner regions of the placenta in close association with fetal blood vessels, with the highest levels of expression in differentiated, syncytial trophoblasts that surround the fetal blood vessels. Thus, it is tempting to speculate that mGCMa is part of the existing cross-regulation between allantoic mesenchyme and extraembryonic ectoderm that is needed to fine-tune the development of the labyrinth layer. Our results point to an induction of mGCMa in chorionic trophoblasts in response to an allantois-derived signal. The existence of such signals has been documented during various phases of placental development. Interaction of the vascular cell adhesion molecule 1 ligand on allantoic mesenchyme with the $\alpha 4$ integrin receptor on chorionic trophoblast, for instance, is an important step during chorion-allantois fusion (12). Later on, both Wnt-2 and HGF/SF are secreted by allantoic mesenchyme and influence development of the labyrinthine trophoblasts (27, 38).

In addition to induction of mGCMa in trophoblasts by allantoic mesenchyme, we postulate a consecutive role for mGCMa in trophoblast differentiation, mediating changes in trophoblast gene expression that allow vasculogenesis and that ultimately lead to the formation of the hemotrichorial barrier around the fetal vessels. Such a model would be compatible with most of our observations. It would explain the localization of mGCMa- and *lacZ*-expressing cells. At the time of chorioallantoic fusion, mGCMa- and *lacZ*-expressing cells would first be confined to the contact zone at the base of the placenta. Later, during the period of active vessel formation, mGCMa- and *lacZ*-expressing cells would spread throughout the labyrinth of the normal placenta and dramatically increase in number concomitant with vasculogenesis. In the mutant placenta, *lacZ*-expressing cells would also appear first at the base of the placenta. Their failure to differentiate in the absence of mGCMa would prevent the allantoic vessels from adequately invading the prospective labyrinth and from expanding. The base of the mutant placenta would remain the only site where chorionic trophoblasts stay in contact with allantoic mesenchyme and would therefore be the only region that contains *lacZ*-expressing trophoblasts in the mutant. This is indeed the case. Because *lacZ* expression is lost in the mutant placenta from 12.5 d.p.c. onwards, we furthermore have to postulate a disappearance of the inducing mesenchymal signal. It is possible that the resorption of the mutant conceptus is the primary cause for this disappearance. Alternatively, the allantois-derived paracrine signal might normally be turned off at this time of development and be replaced by a positive autoregulatory feedback loop as has been shown to exist for *Drosophila* GCM (26). Maintenance of mGCMa expression would then be dependent on mGCMa itself, and absence of mGCMa in the mutant would cause a gradual extinction of mGCMa expression. The existence of an autoregulatory mechanism and the identification of additional downstream targets will be the focus of future experiments and will help us to understand mGCMa function in the placenta. Whether mGCMa has an additional role at later times during development or in the adult will be clarified only once tetraploid rescue experiments have been performed.

ACKNOWLEDGMENTS

J.S., E.R.-S., and D.R. contributed equally to the work.

We thank U. Borgmeyer for providing in situ hybridization probes. T. Mordhorst is acknowledged for expert technical assistance.

This work was supported by a grant from the Deutsche Forschungsgemeinschaft (SFB 444) to M.W.

REFERENCES

1. **Akiyama, Y., T. Hosoya, A. M. Poole, and Y. Hotta.** 1996. The gcm-motif: a novel DNA-binding motif conserved in Drosophila and mammals. Proc. Natl. Acad. Sci. USA **93:**14912–14916.
2. **Akiyama-Oda, Y., T. Hosoya, and Y. Hotta.** 1998. Alteration of cell fate by ectopic expression of *Drosophila glial cells missing* in non-neural cells. Dev. Genes Evol. **208:**578–585.
3. **Altshuller, Y., N. G. Copeland, D. J. Gilbert, N. A. Jenkins, and M. A. Frohman.** 1996. Gcm1, a mammalian homolog of Drosophila glial cells missing. FEBS Lett. **393:**201–204.
4. **Anderson, D. J.** 1995. A molecular switch for the neuron-glia developmental decision. Neuron **15:**1219–1222.
5. **Barak, Y., M. C. Nelson, E. S. Ong, Y. Z. Jones, P. Ruiz-Lozano, K. R. Chien, A. Koder, and R. M. Evans.** 1999. PPAR gamma is required for placental, cardiac, and adipose tissue development. Mol. Cell **4:**585–595.
6. **Basyuk, E., J. C. Cross, J. Corbin, H. Nakayama, P. Hunter, B. Nait-Oumesmar, and R. A. Lazzarini.** 1999. Murine Gcm1 gene is expressed in a subset of placental trophoblast cells. Dev. Dyn. **214:**303–311.
7. **Bernardoni, R., A. A. Miller, and A. Giangrande.** 1998. Glial differentiation does not require a neural ground state. Development **125:**3189–3200.
8. **Bernardoni, R., V. Vivancos, and A. Giangrande.** 1997. glide/gcm is expressed and required in the scavenger cell lineage. Dev. Biol. **191:**118–130.
9. **Dumont, D. J., G. H. Fong, M. C. Puri, G. Gradwohl, K. Alitalo, and M. L. Breitman.** 1995. Vascularization of the mouse embryo: a study of flk-1, tek, tie, and vascular endothelial growth factor expression during development. Dev. Dyn. **203:**80–92.
10. **Gnarra, J. R., J. M. Ward, F. D. Porter, J. R. Wagner, D. E. Devor, A. Grinberg, M. R. Emmert-Buck, H. Westphal, R. D. Klausner, and W. M. Linehan.** 1997. Defective placental vasculogenesis causes embryonic lethality in VHL-deficient mice. Proc. Natl. Acad. Sci. USA **94:**9102–9107.
11. **Guillemot, F., A. Nagy, A. Auerbach, J. Rossant, and A. L. Joyner.** 1994. Essential role of Mash-2 in extraembryonic development. Nature **371:**333–336.
12. **Gurtner, G. C., V. Davis, H. Li, M. J. McCoy, A. Sharpe, and M. I. Cybulsky.** 1995. Targeted disruption of the murine VCAM1 gene: essential role of VCAM-1 in chorioallantoic fusion and placentation. Genes Dev. **9:**1–14.
13. **Hernandez-Verdun, D., and C. Legrand.** 1975. In vitro study of chorionic and ectoplacental trophoblast differentiation in the mouse. J. Embryol. Exp. Morphol. **34:**633–644.
14. **Hogan, B., B. Beddington, F. Constantini, and E. Lacy.** 1994. Manipulating the mouse embryo. Cold Spring Harbor Laboratory Press, Cold Spring Harbor, N.Y.
15. **Hosoya, T., K. Takizawa, K. Nitta, and Y. Hotta.** 1995. glial cells missing: a binary switch between neuronal and glial determination in Drosophila. Cell **82:**1025–1036.
16. **Hunter, P. J., B. J. Swanson, M. A. Haendel, G. E. Lyons, and J. C. Cross.**

1999. Mrj encodes a DnaJ-related co-chaperone that is essential for murine placental development. Development **126:**1247–1258.
17. **Janatpour, M. J., M. F. Utset, J. C. Cross, J. Rossant, J. Dong, M. A. Israel, and S. J. Fisher.** 1999. A repertoire of differentially expressed transcription factors that offers insight into mechanisms of human cytotrophoblast differentiation. Dev. Genet. **25:**146–157.
18. **Jones, B. W., R. D. Fetter, G. Tear, and C. S. Goodman.** 1995. glial cells missing: a genetic switch that controls glial versus neuronal fate. Cell **82:** 1013–1023.
19. **Kammerer, M., B. Pirola, S. Giglio, and A. Giangrande.** 1999. GCMB, a second human homolog of the fly glide/gcm gene. Cytogenet. Cell Genet. **84:**43–47.
20. **Kanemura, Y., S. Hiraga, N. Arita, T. Ohnishi, S. Izumoto, K. Mori, H. Matsumura, M. Yamasaki, S. Fushiki, and T. Yoshimine.** 1999. Isolation and expression analysis of a novel human homologue of the Drosophila glial cells missing (gcm) gene. FEBS Lett. **442:**151–156.
21. **Kim, J., B. W. Jones, C. Zock, Z. Chen, H. Wang, C. S. Goodman, and D. J. Anderson.** 1998. Isolation and characterization of mammalian homologs of the *Drosophila* gene *glial cells missing*. Proc. Natl. Acad. Sci. USA **95:**12364–12369.
22. **Klaes, A., T. Menne, A. Stollwerk, H. Scholz, and C. Klämbt.** 1994. The ETS transcription factors encoded by the Drosophila gene pointed direct glial cell differentiation in the embryonic CNS. Cell **78:**149–160.
23. **Lescisin, K. R., S. Varmuza, and J. Rossant.** 1988. Isolation and characterization of a novel trophoblast-specific cDNA in the mouse. Genes Dev. **2:**1639–1646.
24. **Li, Y., and R. R. Behringer.** 1998. Esx1 is an X-chromosome-imprinted regulator of placental development and fetal growth. Nat. Genet. **20:**309–311.
25. **Luo, J., R. Sladek, J. A. Bader, A. Matthyssen, J. Rossant, and V. Giguere.** 1997. Placental abnormalities in mouse embryos lacking the orphan nuclear receptor ERR-beta. Nature **388:**778–782.
26. **Miller, A. A., R. Bernardoni, and A. Giangrande.** 1998. Positive autoregulation of the glial promoting factor glide/gcm. EMBO J. **21:**6316–6326.
27. **Monkley, S. J., S. J. Delaney, D. J. Pennisi, J. H. Christiansen, and B. J. Wainwright.** 1996. Targeted disruption of the Wnt2 gene results in placentation defects. Development **122:**3343–3353.
28. **Morasso, M. I., A. Grinberg, G. Robinson, T. D. Sargent, and K. A. Mahon.** 1999. Placental failure in mice lacking the homeobox gene Dlx3. Proc. Natl. Acad. Sci. USA **96:**162–167.
29. **Reifegerste, R., J. Schreiber, S. Gulland, A. Ludemann, and M. Wegner.** 1999. mGCMa is a murine transcription factor that overrides cell fate decisions in Drosophila. Mech. Dev. **82:**141–150.
30. **Schmidt, C., F. Bladt, S. Goedecke, V. Brinkmann, W. Zschiesche, M. Sharpe, E. Gherardi, and C. Birchmeier.** 1995. Scatter factor/hepatocyte growth factor is essential for liver development. Nature **373:**699–702.
31. **Schreiber, J., J. Enderich, and M. Wegner.** 1998. Structural requirements for DNA binding of GCM proteins. Nucleic Acids Res. **26:**2337–2343.
32. **Schreiber, J., E. Sock, and M. Wegner.** 1997. The regulator of early gliogenesis Glial Cells Missing is a transcription factor with a novel type of DNA-binding domain. Proc. Natl. Acad. Sci. USA **94:**4739–4744.
33. **Steingrimsson, E., L. Tessarollo, S. W. Reid, N. A. Jenkins, and N. G. Copeland.** 1998. The bHLH-Zip transcription factor Tfeb is essential for placental vascularization. Development **125:**4607–4616.
34. **Süsens, U., J. B. Aguiluz, R. M. Evans, and U. Borgmeyer.** 1997. The germ cell nuclear factor mGCNF is expressed in the developing nervous system. Dev. Neurosci. **19:**410–420.
35. **Tanaka, M., M. Gertsenstein, J. Rossant, and A. Nagy.** 1997. Mash2 acts cell autonomously in mouse spongiotrophoblast development. Dev. Biol. **190:** 55–65.
36. **Tuerk, E. E., J. Schreiber, and M. Wegner.** 2000. Protein stability and domain topology determine the transcriptional activity of the mammalian Glial Cells Missing homolog, GCMb. J. Biol. Chem. **275:**4774–4782.
37. **Tybulewicz, V. L., C. E. Crawford, P. K. Jackson, R. T. Bronson, and R. C. Mulligan.** 1991. Neonatal lethality and lymphopenia in mice with a homozygous disruption of the c-abl proto-oncogene. Cell **65:**1153–1163.
38. **Uehara, Y., O. Minowa, C. Mori, K. Shiota, J. Kuno, T. Noda, and N. Kitamura.** 1995. Placental defect and embryonic lethality in mice lacking hepatocyte growth factor/scatter factor. Nature **373:**702–705.
39. **Vincent, S., J.-L. Vonesch, and A. Giangrande.** 1996. glide directs glial fate commitment and cell fate switch between neurones and glia. Development **122:**131–139.
40. **Wendling, O., P. Chambon, and M. Mark.** 1999. Retinoid X receptors are essential for early mouse development and placentogenesis. Proc. Natl. Acad. Sci. USA **96:**547–551.
41. **Wilkinson, D. G.** 1992. In situ hybridization: a practical approach. Oxford University Press-IRL Press, Oxford, United Kingdom.
42. **Yang, J. T., H. Rayburn, and R. O. Hynes.** 1995. Cell adhesion events mediated by alpha 4 integrins are essential in placental and cardiac development. Development **121:**549–560.